FDX1 inhibits thyroid cancer malignant progression by inducing cuprotosis

Gaoxiang Chen [*], Jianan Zhang, Weifeng Teng, Yong Luo, Xiaochun Ji

Department of Thyroid and Breast Surgery, Ningbo Medical Center Lihuili Hospital, No.57 XingNing Road, Ningbo, Zhejiang Province, China

ARTICLE INFO

ABSTRACT

Cuprotosis is a recently identified cell death form that caused by intracellular copper accumulation and regulated by FDX1. This work aimed to explore the role of cuprotosis and the pivotal regulatory gene FDX1 in thyroid cancer development. We observed that expression of FDX1 in tumor section was notably lower than that in non-tumor sections in clinical samples. Induction of cuprotosis by elesclomol (ES) significantly repressed the in vitro and in vivo growth of thyroid cancer cells, simultaneously elevated Cu level and expression of FDX1, whereas depletion of FDX1 abolished these effects. Knockdown of FDX1 decreased the lipoylation level of DLAT and DLST in thyroid cancer cells, alleviated cuprotosis-induced cell death, simultaneously upregulated the levels of PA and α-KG. These findings demonstrated that FDX1 promotes the cuprotosis of thyroid cancer cells via regulating the lipoylation of DLAT.

1. Introduction

Cell death involves a series of signaling cascades and molecular mechanisms [1]. For example, apoptosis, necrotic apoptosis, pyroptosis and ferroptosis are corelated with the level and functions of multiple proteins and lipids [2,3]. Elesclomol (ES) has previously been reported to induce Ros-dependent apoptosis, yet ES-induced cell death does not involve activation and cleavage of caspase 3 (the biomarker of apoptosis) [4]. Besides, the cytotoxicity of ES remains unaffected when cells were treated with inhibitors of known cell death mechanisms, including ferroptosis (ferrostatin-1), necrosis (necrostatin-1), and oxidative stress (N-acetyl cysteine), implying the different mechanisms involved in copper ionophores [5,6].

Copper ionophores are small molecules interact with copper and can shuttle copper into cells, hence are thought of useful tools for studying copper toxicity [7,8]. Accumulating evidence suggest that the mechanisms of copper ionophores induced cell death involve accumulation of intracellular copper rather than the effects of small molecular themselves [9,10]. Studies on revealed that copper ionophores with different structures that bind copper share the same killing profiles in hundreds of cell lines [5,11]. Further analyses on structure-function relationship showed that modifications that eliminating the copper-binding ability of these compounds or administration of copper chelation resulted in loss of cell cytotoxicity of the compounds [5]. These studies indicate that copper ionophores induced cell death mainly depends on intracellular copper accumulation.

Golub and colleagues reported that copper induces cell death by targeting lipoylated tricarboxylic acid (TCA) cycle proteins, which identified FDX1, a key gene that promotes copper induced death [12]. This new form of cell death induced by copper ionophores was then named as Cuprotosis, which opened a new area of cell death mechanism research. However, the role of cuprotosis and the pivotal

---

regulatory gene FDX1 in thyroid cancer has not been determined. In this work, we evaluated the expression of FDX1 in collected clinical samples of thyroid cancer and measured the changes of cell viability and cuprotosis upon alteration of FDX1 to explore the mechanisms of FDX1-mediated cuprotosis in thyroid cancer development.

2. Materials and methods

2.1. Cell culture

The thyroid cancer cell lines TPC-1, HTH83, BCPAP and KAT-5 and the normal human thyroid cell line MTHY-ORI3.1 were bought from American Type Culture Collection and Wuhan Procell. All cells were incubated in RPMI 1640 that supplemented with 10% FBS at 37 °C incubator.

2.2. Cell treatment and transfection

Cells were incubated in 6-well plates and treated with 20 nM elesclomol (ES; MCE) for 24 h and collected for following experiments. For cell transfection, the siFDX1 and siDLAT were bought from GenePharma (China) and transfected into cells using Lipofectamine 2000 (Invitrogen, USA) following the manufacturer's introduction.

2.3. Cell viability and proliferation

Cell viability and proliferation were measured by cell counting kit-8 (CCK-8, SolarBio, China) and colony formation assay. In brief, cells that transfected with indicated siRNA were seeded into 96-well plates and treated with ES for 24, 48, 72 h, respectively. Then CCK-8 reagent was added for another 2-h-incubation. The optical density was measured at 450 nm and calculated for viability.

For colony formation, cells were suspended as single cells and seeded into 6-well plate. After incubation for 10 days, the colonies were stained with crystal violet for 20 min and captured under light microscope (Leica, Germany).

2.4. Western blotting assay

Total proteins were obtained from cells using RIPA buffer (Beyotime, China) and quantified using BCA Protein Assay Kit (Beyotime, China). Then identical quantities of proteins were divided by SDA-PAGE gels and blotted onto PVDF membranes (Millipore, USA). After blocking in 5% non-fat milk and incubation with primary antibodies against FDX1 (1:1000, Abcam, USA), Lip-DLAT (1:1000, Abcam, USA), lip-DLST (1:1000, Abcam, USA), DLAT (1:1000, Abcam, USA), DLST (1:1000, Abcam, USA), or β-actin (1:1000, Abcam, USA) at 4 °C overnight, the blots were hatched with Goat anti-Mouse or anti-Rabbit IgG secondary antibody (1:1000, Abcam, USA). After reaction with ECL reagent, the blots were visualized under a gel imaging system.

2.5. Quantitative real time PCR (qPCR)

Total RNA was harvested using the Trizol reagent (Thermo, USA) and subjected to reverse transcription using the HiScript III RT SuperMix for qPCR kit (Vazyme). The qPCR was performed using a SYBR qPCR Master Mix (Vazyme, China). GAPDH was adopted as an internal control for the quantification of indicated genes.

FDX1 forward primer: 5'- CTTTGGAGTCTCTCGCGGC-3'; FDX1 reverse primer: 5'- CTCTGCCTTCACCCACATCA-3';

2.6. Immunofluorescence (IF) experiment

To detect the level of DLAT, thyroid cancer cells were transfected with siRNAs and seeded into confocal dishes. Cells were then fixed with 4% PFA and incubated with anti-DLAT antibody (CST, USA) overnight at 4 °C, followed by incubation with Alexa Fluor 633 secondary antibody. The images were then captured under the confocal laser scanning microscope (Leica, Germany).

2.7. Detection of Cu, pyruvate acid (PA) and α-ketoglutarate dehydrogenase (α-KG)

The levels of Cu, PA, and α-KG were measured using commercial kits including Cu detection kit (Elabscience, China), CheKine PA detection kit (Abbkine, China, Alpha Ketoglutarate (alpha KG) Assay Kit (Abcam, USA)) according to manufacturer's protocols.

2.8. Xenograft mouse model

Male Balb/C nude mice that aged 4–6 weeks old were bought from Vital River Laboratory (Beijing, China) and fed for one week to acclimate. TPC-1 cells that transfected with siFDX1 were digested and suspended in saline, then 50 μl saline that contains 5×10^6 cells were subcutaneously injected into the fat pad of each mouse. The mice were then fed for 30 days, during which the length and width of tumors were measured every 5 days and tumor volume were calculated. The mice were then sacrificed, and tumors were collected and weighed. All experiments were approved by the Animal Experiment Ethic Committee of Ningbo Medical Center Lihuili Hospital.

2.9. Patient samples measurement

Patients (n = 18) with thyroid cancer were recruited in this study and have signed informed consents. No patients received chemotherapy or radiotherapy prior to surgery. The tumors and adjacent non-tumor tissues were resected from patients during surgery. The collected tissues were conserved in liquid nitrogen or fixed in 4% PFA for qPCR or histological analysis, respectively. Total RNAs were extracted from frozen tissues and RNA level of FDX1 was measured using qPCR assay. The protein level of FDX1 in tissues were measured by immunohistochemical (IHC) analysis using anti-FDX1 antibody.

2.10. Statistics

Data in this work were analyzed using the GraphPad Prism 7.0 Software. For comparison, two-sided Student's t-test and one-way ANOVA followed by Dunnett's multiple comparisons test. P < 0.05 was regarded as statistically significant.
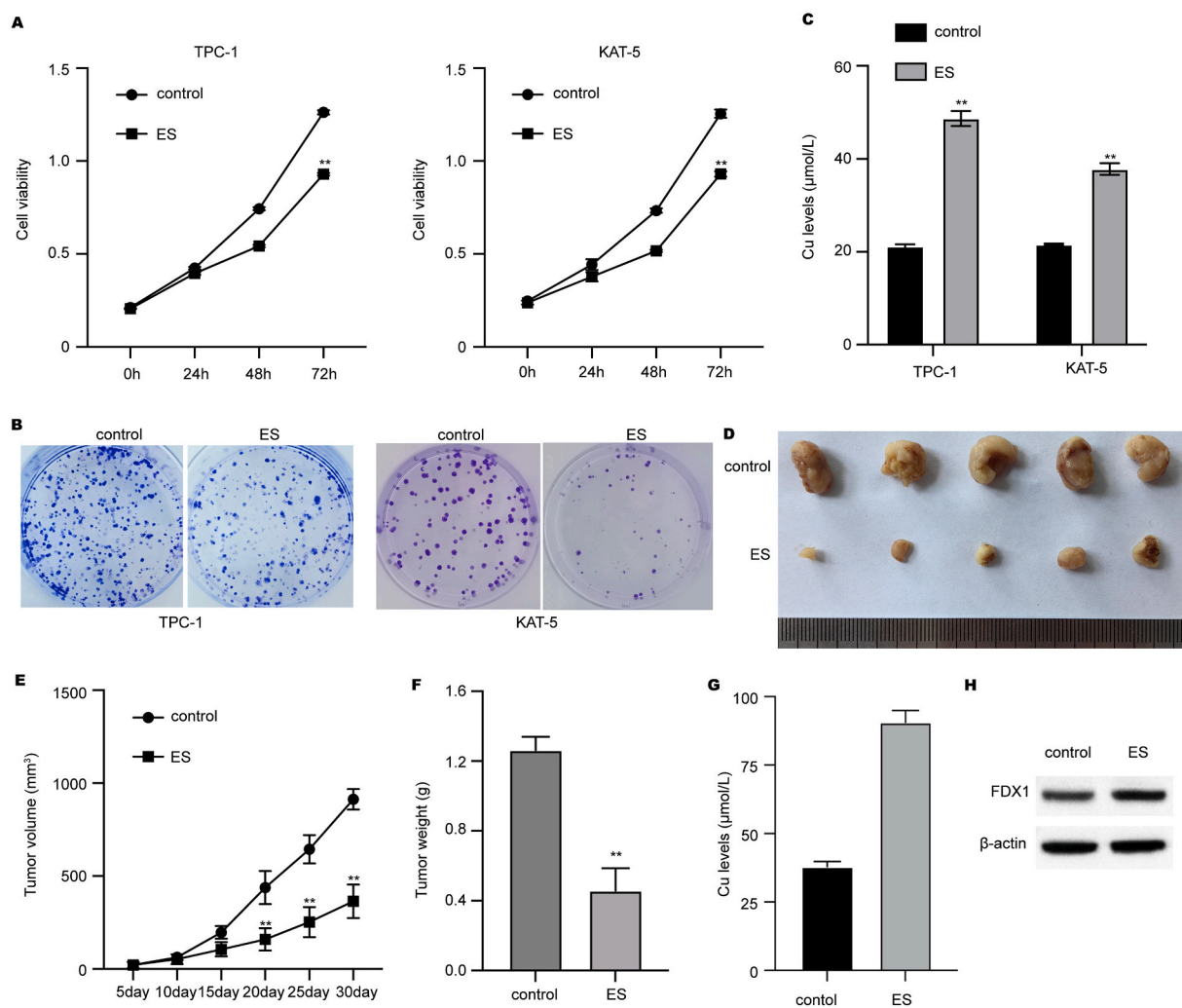

Fig. 1. Cuprotosis inducer suppresses growth of thyroid cancer cells in vitro and in vivo. (A–C) Thyroid cancer cell lines TPC-1 and KAT-5 were treated with elesclomol (ES). Then (A) cell viability, (B) cell proliferation, and (C) level of Cu were measured by CCK-8, colony formation, and commercial kit, respectively. (D–F) In vivo xenograft mouse model was established using TPC-1 cells and treated with ES. Then (D) tumor size, (E) tumor growth curve, and (F) tumor weight was recorded. (G) Cu level in tumor tissues. (H) Protein expression of FDX1 in tumor tissues was measured by western blotting. **p < 0.01.

3. Results

3.1. Cuprotosis inducer suppresses growth of thyroid cancer cells in vitro and in vivo

The elesclomol (ES), inducer of cuprotosis, significantly suppressed the growth of thyroid cancer cell lines (TPC-1 and KAT-5) within 72 h (Fig. 1A). The results from colony formation revealed decreased proliferation of thyroid cancer cells under ES treatment (Fig. 1B). Moreover, we observed remarkably increased level of Cu after ES treatment in thyroid cancer cells (Fig. 1C). The results from xenograft model also presented smaller tumor size (Fig. 1D), suppressed tumor growth (Fig. 1E), and decreased tumor weight (Fig. 1F) of thyroid cancer cells in ES group compared with control group. Moreover, we observed that ES treatment increased the Cu level (Fig. 1G) and increased FDX1 expression (Fig. 1H) in xenograft tumors compared with the control groups.

3.2. FDX1 is downregulated in thyroid cancer

FDX1 is reported as a mediator of cuprotosis. Here, we evaluated the expression of FDX1 in thyroid cancer tissues and cell lines. As shown in Fig. 2A and B, the expression of FDX1 in clinical tumors samples from thyroid cancer was notably decreased compared with paired non-tumor tissues. Moreover, the expression of FDX1 in thyroid cancer cell lines, including the TPC-1, HTH83, BCPAP and KAT-5, were notably lower than that in normal cell line MTHY-ORI3.1 (Fig. 2C). These data indicated that FDX1 in downregulated in thyroid cancer.

3.3. FDX1 mediates the cuprotosis in thyroid cancer cells

Subsequently, we examined the role of FDX1 in ES-induced cuprotosis of thyroid cancer cells. Ectopic expression or transfection with siFDX1 could effectively upregulate or suppress the expression of FDX1 in thyroid cancer cells (Fig. 3A). The results from CCK-8 and colony formation assay demonstrated that depletion of FDX1 notably recovered viability and proliferation of thyroid cancer cells that treated with ES (Fig. 3B and C). Consistently, the in vivo growth of thyroid that suppressed by ES was also reversed by depletion of FDX1 (Fig. 3D). Treatment with ES elevated the Cu level in xenograft tumors, which was repressed by knockdown of FDX1.

3.4. FDX1 regulates the lipoylation of DLST in thyroid cancer cells

To investigate the mechanisms underlying FDX1 regulated cuprotosis, we examined the lipoylation of DLAT and DLST in thyroid cancer cells. The lipoylation of DLAT and DLST were notably suppressed by siFDX1 in thyroid cancer cells (Fig. 4A). Images from confocal microscope indicated that depletion of FDX1 led to decreased foci of DLAT in thyroid cells (Fig. 4B). Moreover, the accumulation of pyruvate acid (PA) and a-ketoglutarate dehydrogenase (α-KG) were notably elevated in siFDX1-transfected cells (Fig. 4C), owing to the inhibition of TCA and compromised protein lipoylation. Next, we investigated whether DLAT mediate the FDX1 regulated cuprotosis and metabolism. As shown in Fig. 4D, ES treatment induced cell death (Fig. 4D) and decreased levels of PA and α-KG (Fig. 4E) and siFDX1 abolished the effects of ES, whereas overexpression of DLAT1 repressed proliferation and accumulation of PA and α-KG. These data indicated that FDX1 regulates the lipoylation of DLST to induce cuprotosis in thyroid cancer cells.

4. Discussion

In this study, we investigated the cuprotosis of thyroid cancer and explored the effects of FDX1 in this process. We demonstrated
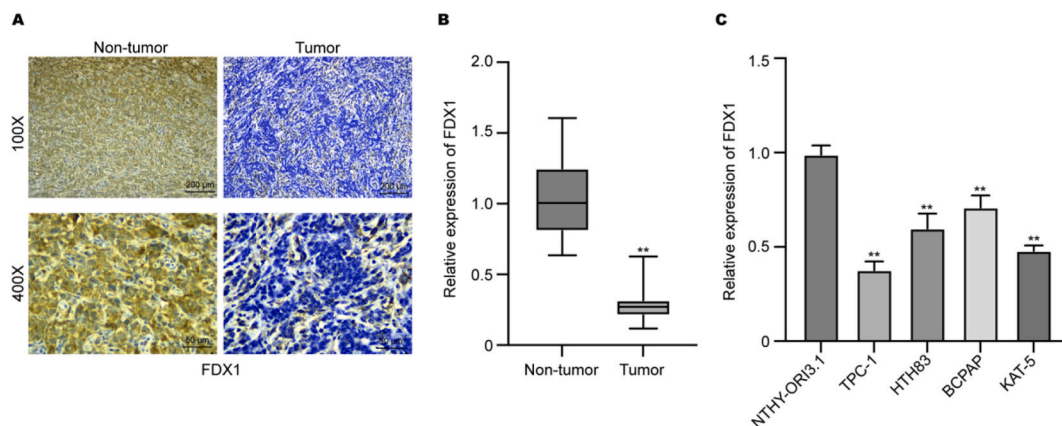

Fig. 2. FDX1 is downregulated in thyroid cancer. (A and B) The clinical tumor tissues and paired non-tumor tissues were collected from patients with thyroid cancer, then expression of FDX1 was measured using (A) IHC and (B) qPCR experiments. (C) The RNA level of FDX1 in thyroid cancer cell lines (TPC-1, HTH83, BCPAP and KAT-5) and normal cell line MTHY-ORI3.1 was measured by qPCR assay. **$p < 0.01$.
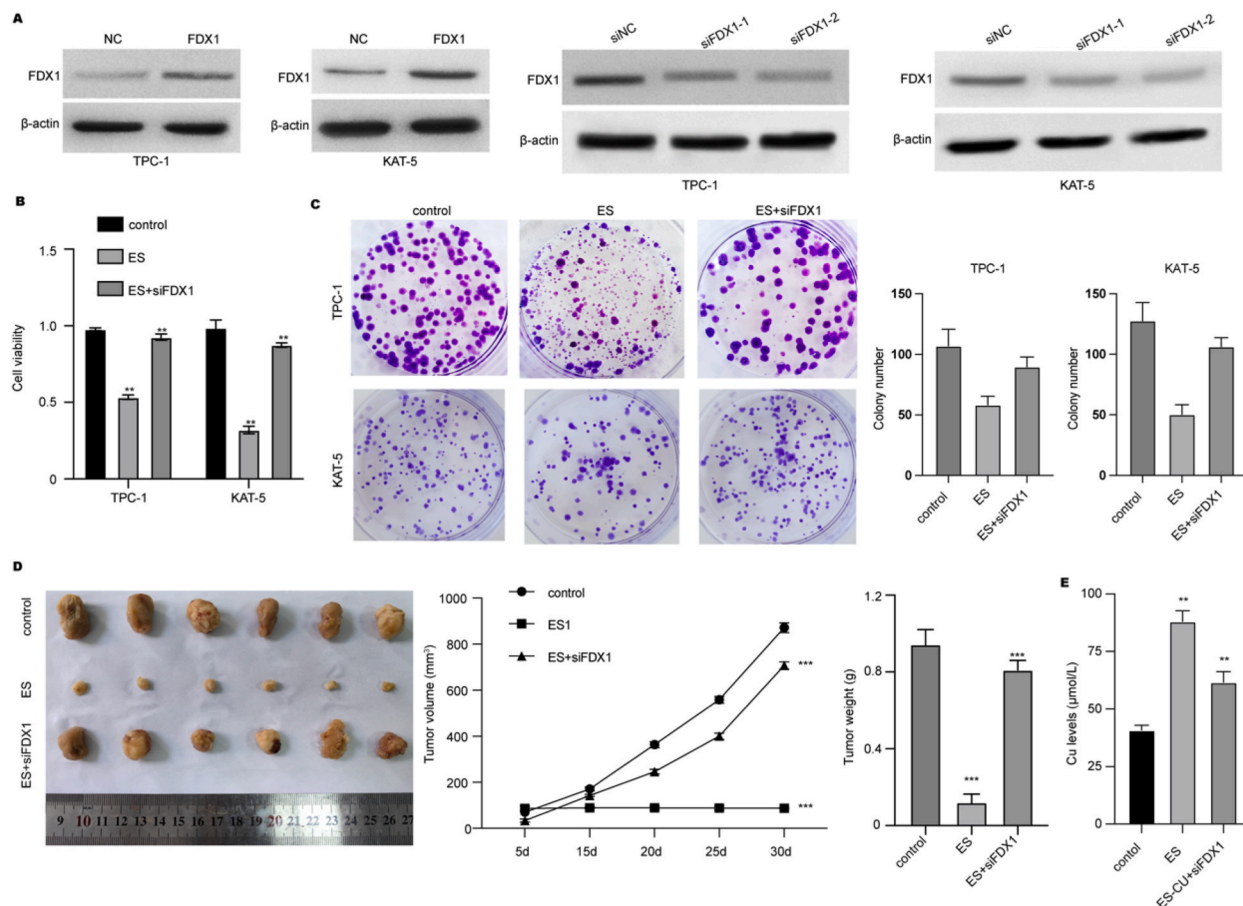
Fig. 3. FDX1 mediates the cuprotosis in thyroid cancer cells. (A–C) Thyroid cancer cells were transfected with FDX1 overexpression vectors or siFDX1. (A) Protein level of FDX1 in cells was measured by western blotting assay. Control: untreated group; NC: negative control. (B) Cell viability was measured by CCK-8. (C) Cell proliferation was detected using colony formation. (D) In vivo xenograft mouse model was established using TPC-1 cells and treated with ES and siFDX1. Then tumor size, tumor growth curve, and tumor weight were recorded. (E) Cu level in tumor tissues. **p < 0.01.

that the treatment with ES notably induced the intracellular accumulation of Cu and caused cell death, whereas knockdown of FDX1 could abolish these effects. In normal condition, intracellular copper concentrations are kept at extraordinarily low levels by active homeostatic mechanisms that work across concentration gradients to prevent the accumulation of free intracellular copper that is detrimental to cells [13,14]. Upon the induction by copper ionophores, the mitochondria respiration process is changed for cuprotosis, and that copper does not target the electron transport chain directly but rather components of the tricarboxylic acid (TCA) cycle [12]. Studies revealed that the loss of FDX1, the Fe–S cluster protein, disrupted the lipoylation of certain proteins, including DLAT and S-succinyltransferase (DLST). And when protein lipoylation is abrogated by knockdown of FDX1, DLST and DLAT loss the binding ability to copper, therefore affects cuprotosis progression.

FDX1 encodes a reductase known to reduce Cu^{2+} to its more toxic form, Cu^{1+}, and to be a direct target of elesclomol [15,16]. Knockdown of FDX1 could rescue the ES-induced cell death [17]. Gene knockdown study also confirmed that depletion of FDX1 and lipoyl synthase conferred resistance of cells to copper-induced death [18], further emphasized the functional link between the protein lipoylation machinery and copper toxicity. Here, we observed impaired lipoylation of DLAT in thyroid cancer cells upon depletion of FDX1, implying the potential regulatory axis of FDX1-DLAT.

Protein lipoylation is a highly conserved lysine posttranslational modification that is known to occur on only four enzymes, including the DLAT and DLST [19]. These enzymes are all involved in the metabolic complexes that regulation the entry of carbon to TCA cycle [20,21]. And lipoylation of these enzymes is identified as essential process for their catalytic function [21].

Moreover, previous study has indicated that protein lipoylation would be compromised upon inhibition of the TCA cycle at pyruvate dehydrogenase (PDH) complex, including the DLAT, pyruvate dehydrogenase E1 subunit alpha 1, and pyruvate dehydrogenase E1 subunit beta [20], and a-ketoglutarate dehydrogenase [22]. Furthermore, metabolite profiling under knockdown of FDX1 led to an accumulation of PA and α-KG [12]. Consistent with these articles, we also observed elevated levels of PA and α-KG upon FDX1 depletion in ES-treated thyroid cancer cells. However, several limitations exist in current study, such as the lack of exploration on the connection between FDX1 with the tumor microenvironment. Also, further examination of altered metabolic markers upon change of
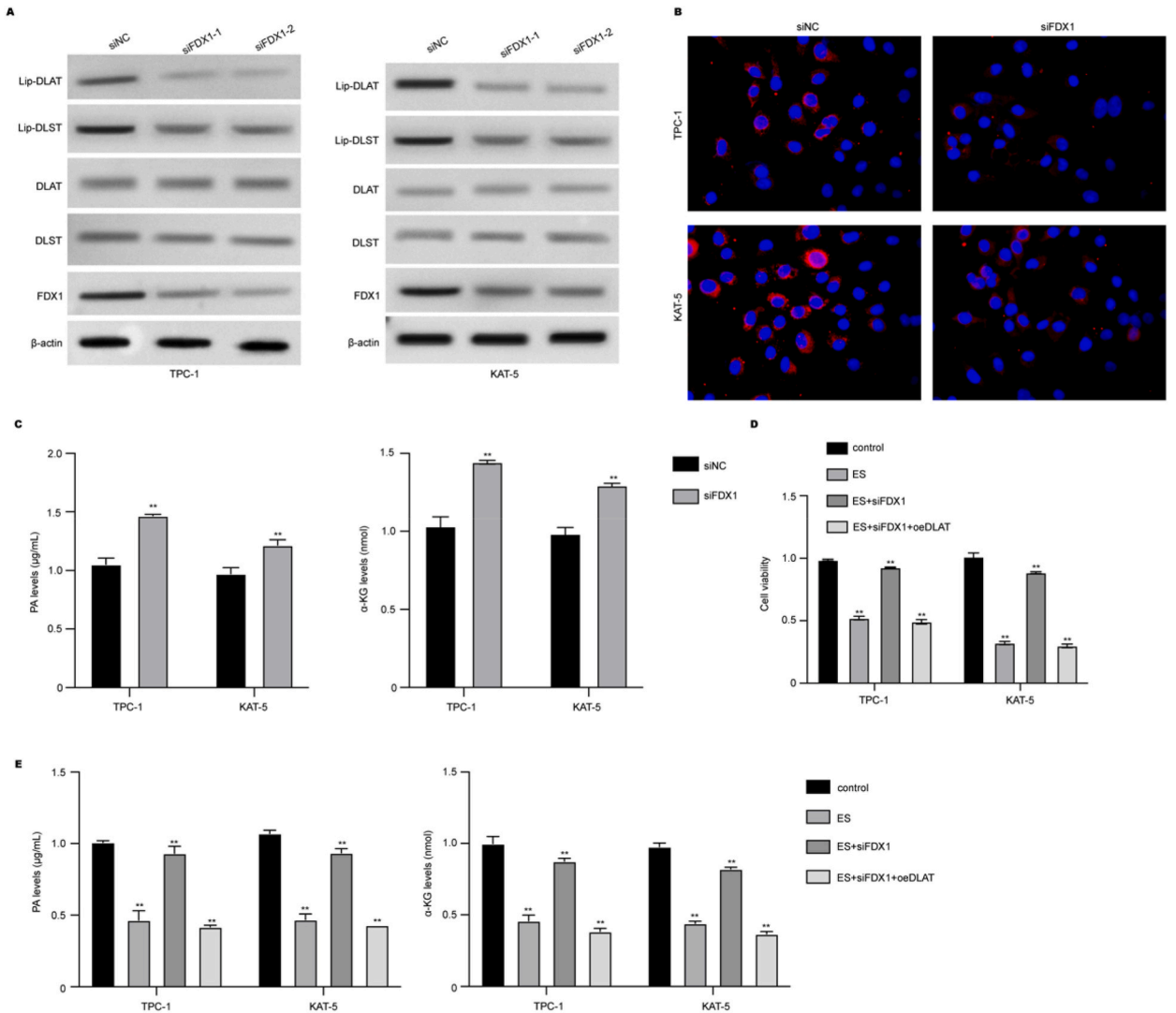
Fig. 4. FDX1 regulates the lipoylation of DLST in thyroid cancer cells. (A) Protein levels of Lip-DLAT, lip-DLST, DLAT, DLST, FDX1 in thyroid cancer cells were measured by western blotting assay. (B) Immunofluorescence imaging of DLAT (Blue, DAPI; Red, DLAT) in thyroid cancer cells. (C) The levels of pyruvate acid (PA) and a-ketoglutarate dehydrogenase (α-KG) in thyroid cancer cells under siFDX1 transfection. (D and E) Thyroid cancer cells were treated with ES and transfected with siFDX1 or siDLAT. (D) The cell viability was measured by CCK-8. (E) The levels of PA and α-KG were measured. Control: untreated group; NC: negative control; siNC: siRNA negative control; oeFDX1: FDX1 overexpression. **p < 0.01.

FDX1 should be performed.

5. Conclusion

To summarize, FDX1 is downregulated in tumor tissues of thyroid cancer patients and promotes the cuprotosis of thyroid cancer cells via inducing the lipoylation of DLAT. Our findings highlighted novel molecular mechanisms of thyroid cancer development and may provide a promising target for thyroid cancer therapy.

Author contribution statement

Gaoxiang Chen: Conceived and designed the experiments; Performed the experiments; Analyzed and interpreted the data; Wrote the paper.

Jianan Zhang, Weifeng Teng: Performed the experiments.

Yong Luo: Analyzed and interpreted the data.

Xiaochun Ji: Conceived and designed the experiments; Wrote the paper.

Funding statement

Data availability statement

No data was used for the research described in the article.

Declaration of competing interest

The authors declare that they have no known competing financial interests or personal relationships that could have appeared to influence the work reported in this paper.

References

[1] M.S. D'Arcy, Cell death: a review of the major forms of apoptosis, necrosis and autophagy, Cell Biol. Int. 43 (6) (2019) 582–592, https://doi.org/10.1002/cbin.11137.
[2] S.F. Santagostino, C.A. Assenmacher, J.C. Tarrant, A.O. Adedeji, E. Radaelli, Mechanisms of regulated cell death: current perspectives, Vet. Pathol. 58 (4) (2021) 596–623, https://doi.org/10.1177/03009858211005537.
[3] R.F. Schwabe, T. Luedde, Apoptosis and necroptosis in the liver: a matter of life and death, Nat. Rev. Gastroenterol. Hepatol. 15 (12) (2018) 738–752, https://doi.org/10.1038/s41575-018-0065-y.
[4] L.M. Guthrie, S. Soma, S. Yuan, A. Silva, M. Zulkifli, T.C. Snavely, et al., Elesclomol alleviates Menkes pathology and mortality by escorting Cu to cuproenzymes in mice, Science 368 (6491) (2020) 620–625, https://doi.org/10.1126/science.aaz8899.
[5] P. Zheng, C. Zhou, L. Lu, B. Liu, Y. Ding, Elesclomol: a copper ionophore targeting mitochondrial metabolism for cancer therapy, J. Exp. Clin. Cancer Res. 41 (1) (2022) 271, https://doi.org/10.1186/s13046-022-02485-0.
[6] W. Gao, Z. Huang, J. Duan, E.C. Nice, J. Lin, C. Huang, Elesclomol induces copper-dependent ferroptosis in colorectal cancer cells via degradation of ATP7A, Mol. Oncol. 15 (12) (2021) 3527–3544, https://doi.org/10.1002/1878-0261.13079.
[7] H. Li, P. Yang, J. Wang, J. Zhang, Q. Ma, Y. Jiang, et al., HLF regulates ferroptosis, development and chemoresistance of triple-negative breast cancer by activating tumor cell-macrophage crosstalk, J. Hematol. Oncol. 15 (1) (2022) 2, https://doi.org/10.1186/s13045-021-01223-x.
[8] V. Oliveri, Selective targeting of cancer cells by copper ionophores: an overview, Front. Mol. Biosci. 9 (2022), 841814, https://doi.org/10.3389/fmolb.2022.841814.
[9] P.M. Meggyesy, S. Masaldan, S.A.S. Clatworthy, I. Volitakis, D.J. Eyckens, K. Aston-Mourney, et al., Copper ionophores as novel antiobesity therapeutics, Molecules 25 (21) (2020), https://doi.org/10.3390/molecules25214957.
[10] Y. Li, Copper homeostasis: emerging target for cancer treatment, IUBMB Life 72 (9) (2020) 1900–1908, https://doi.org/10.1002/iub.2341.
[11] M. Buccarelli, Q.G. D'Alessandris, P. Matarrese, C. Mollinari, M. Signore, A. Cappannini, et al., Elesclomol-induced increase of mitochondrial reactive oxygen species impairs glioblastoma stem-like cell survival and tumor growth, J. Exp. Clin. Cancer Res. 40 (1) (2021) 228, https://doi.org/10.1186/s13046-021-02031-4.
[12] P. Tsvetkov, S. Coy, B. Petrova, M. Dreishpoon, A. Verma, M. Abdusamad, et al., Copper induces cell death by targeting lipoylated TCA cycle proteins, Science 375 (6586) (2022) 1254–1261, https://doi.org/10.1126/science.abf0529.
[13] M. Araya, M. Olivares, F. Pizarro, M. González, H. Speisky, R. Uauy, Copper exposure and potential biomarkers of copper metabolism, Biometals 16 (1) (2003) 199–204, https://doi.org/10.1023/a:1020723117584.
[14] T. Skjørringe, L.B. Møller, T. Moos, Impairment of interrelated iron- and copper homeostatic mechanisms in brain contributes to the pathogenesis of neurodegenerative disorders, Front. Pharmacol. 3 (2012) 169, https://doi.org/10.3389/fphar.2012.00169.
[15] Z. Zhang, Y. Ma, X. Guo, Y. Du, Q. Zhu, X. Wang, et al., FDX1 can impact the prognosis and mediate the metabolism of lung adenocarcinoma, Front. Pharmacol. 12 (2021), 749134, https://doi.org/10.3389/fphar.2021.749134.
[16] J. Zhang, X. Kong, Y. Zhang, W. Sun, J. Wang, M. Chen, et al., FDXR regulates TP73 tumor suppressor via IRP2 to modulate aging and tumor suppression, J. Pathol. 251 (3) (2020) 284–296, https://doi.org/10.1002/path.5451.
[17] P. Tsvetkov, A. Detappe, K. Cai, H.R. Keys, Z. Brune, W. Ying, et al., Mitochondrial metabolism promotes adaptation to proteotoxic stress, Nat. Chem. Biol. 15 (7) (2019) 681–689, https://doi.org/10.1038/s41589-019-0291-9.
[18] K. Birsoy, T. Wang, W.W. Chen, E. Freinkman, M. Abu-Remaileh, D.M. Sabatini, An essential role of the mitochondrial electron transport chain in cell proliferation is to enable aspartate synthesis, Cell 162 (3) (2015) 540–551, https://doi.org/10.1016/j.cell.2015.07.016.
[19] N. Shen, S. Korm, T. Karantanos, D. Li, X. Zhang, E. Ritou, et al., DLST-dependence dictates metabolic heterogeneity in TCA-cycle usage among triple-negative breast cancer, Commun Biol 4 (1) (2021) 1289, https://doi.org/10.1038/s42003-021-02805-8.
[20] A. Solmonson, R.J. DeBerardinis, Lipoic acid metabolism and mitochondrial redox regulation, J. Biol. Chem. 293 (20) (2018) 7522–7530, https://doi.org/10.1074/jbc.TM117.000259.
[21] E.A. Rowland, C.K. Snowden, I.M. Cristea, Protein lipoylation: an evolutionarily conserved metabolic regulator of health and disease, Curr. Opin. Chem. Biol. 42 (2018) 76–85, https://doi.org/10.1016/j.cbpa.2017.11.003.
[22] M. Ni, A. Solmonson, C. Pan, C. Yang, D. Li, A. Notzon, et al., Functional assessment of lipoyltransferase-1 deficiency in cells, mice, and humans, Cell Rep. 27 (5) (2019) 1376–1386 e6, https://doi.org/10.1016/j.celrep.2019.04.005.